Università degli Studi della Campania *Luigi Vanvitelli*

PROMETH2O

20IND06 PROMETH2O - Final Workshop

# Next-generation trace water sensors and analyzers for the industry

**Livio Gianfrani**

Dipartimento di Matematica e Fisica, Università degli Studi della Campania Luigi Vanvitelli

**Tuesday 30th of January 2024**

EMPIR EURAMET

The EMPIR initiative is co-funded by the European Union's Horizon 2020 research and innovation programme and the EMPIR Participating States

# The aim of WP1

## *C1 WP1: Improved trace water measurement methods and techniques*

The aim of this work package is to improve trace water measurement methods and techniques in the water fraction between 5 ppm and 5 ppb (equivalently to between -65 °C and -105 °C frost point temperature). The target relative uncertainty for the measurements is between 3 % and 8 % for water concentrations of 5 ppm and 5 ppb, respectively. Sensor performance for different gas species, at various pressures and over time remains a challenge for many applications. Optically based methods can have fast response and can be used with well-defined gas matrices but are prone to interferences from other gases if they suddenly appear in a process. Therefore, it is vital that sensors can handle possible interferences while keeping their high selectivity for target species.

- CC-FS-CRDS in the NIR
- Far-UV absorption spectroscopy
- Conventional FTIR-based spectroscopy
- Cavity-enhanced frequency-modulated spectroscopy

## C1 WP1: Improved trace water measurement methods and techniques

The aim of this work package is to improve trace water measurement methods and techniques in the water fraction between 5 ppm and 5 ppb (equivalently to between -65 °C and -105 °C frost point temperature). The target relative uncertainty for the measurements is between 3 % and 8 % for water concentrations of 5 ppm and 5 ppb, respectively. Sensor performance for different gas species, at various pressures and over time remains a challenge for many applications. Optically based methods can have fast response and can be used with well-defined gas matrices but are prone to interferences from other gases if they suddenly appear in a process. Therefore, it is vital that sensors can handle possible interferences while keeping their high selectivity for target species.

- CC-FS-CRDS in the NIR
- Far-UV absorption spectroscopy
- Conventional FTIR-based spectroscopy
- Cavity-enhanced frequency-modulated spectroscopy

✓ Principle of operation
✓ Description
✓ Test and performance

# The CRDS principle

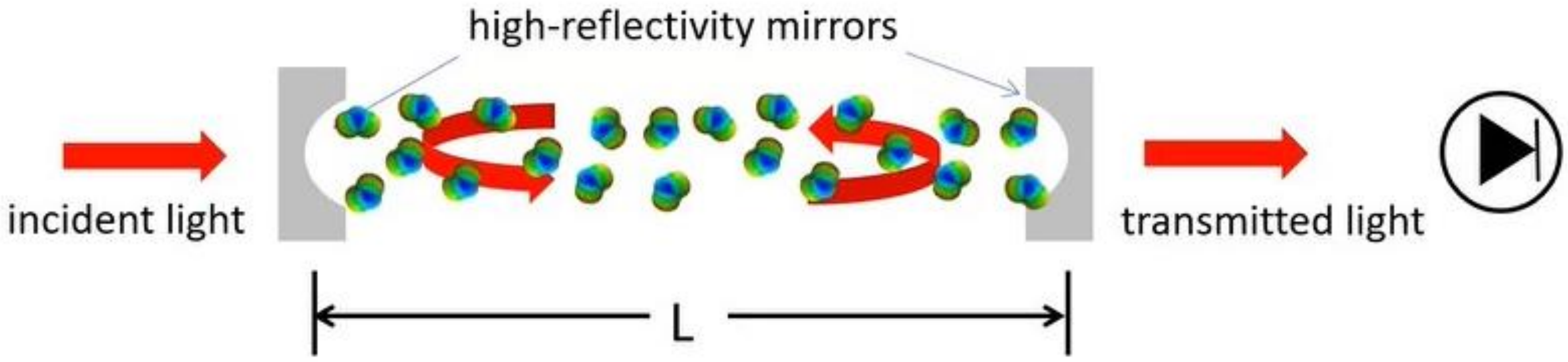


**Properties:**

- ✓ Resonances occur at multiples of $c/2L$ = FSR
- ✓ These resonances have kHz-level width and therefore act as optical frequency filters
- ✓ The optical pathlength is enhanced by a factor $2F/\pi$
- ✓ The optical power is enhanced as well

# The CRDS principle

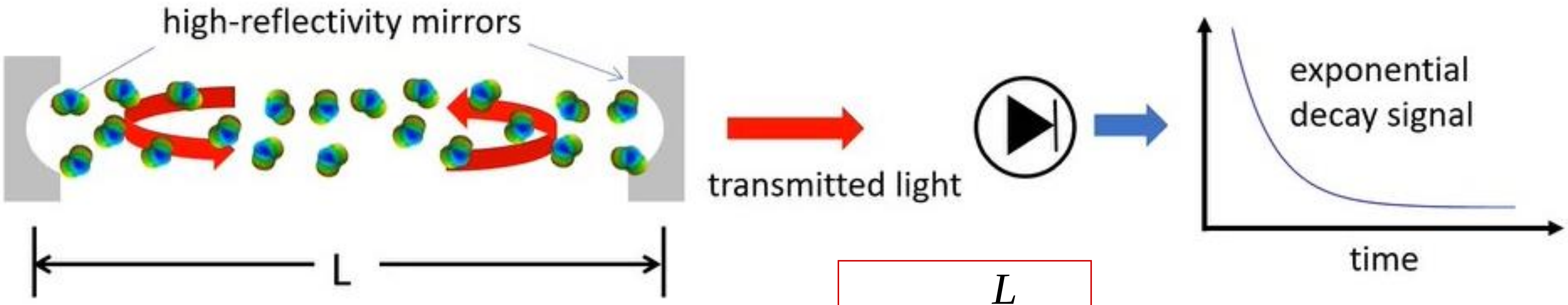


$$\tau_o = \frac{L}{c(1-R)}$$

$$\tau(\nu) = \frac{L}{c[(1-R)+\alpha(\nu)L]} \;\Rightarrow\; \alpha(\nu) = \frac{\tau_0 - \tau}{c\tau_0\tau}$$

**Properties:**

- ✓ Resonances occur at multiples of c/2L = FSR
- ✓ These resonances have kHz-level width and therefore act as optical frequency filters
- ✓ The optical pathlength is enhanced by a factor $2F/\pi$
- ✓ The optical power is enhanced as well

**Main advantages:**

- ➢ Intrinsic insensitivity to laser intensity fluctuations
- ➢ Absolute nature of the absorption measurement
- ➢ Traceability to SI standards (time and frequency)

# The CC-FS-CRDS spectrometer

$\lambda$ = **1.3947 μm**

**Wavenumber:**
7170.27781 cm$^{-1}$

**$H_2O$ line:**
$3_{2,2} \rightarrow 2_{2,1}$
$\nu_1 + \nu_3$ band

**Cavity details:**
Plano-concave mirrors;
R=99.9994%;
Finesse ≃ 500000
Cavity-spacer in 316L-type stainless steel with an electro-polished inner surface;
L≃50 cm.

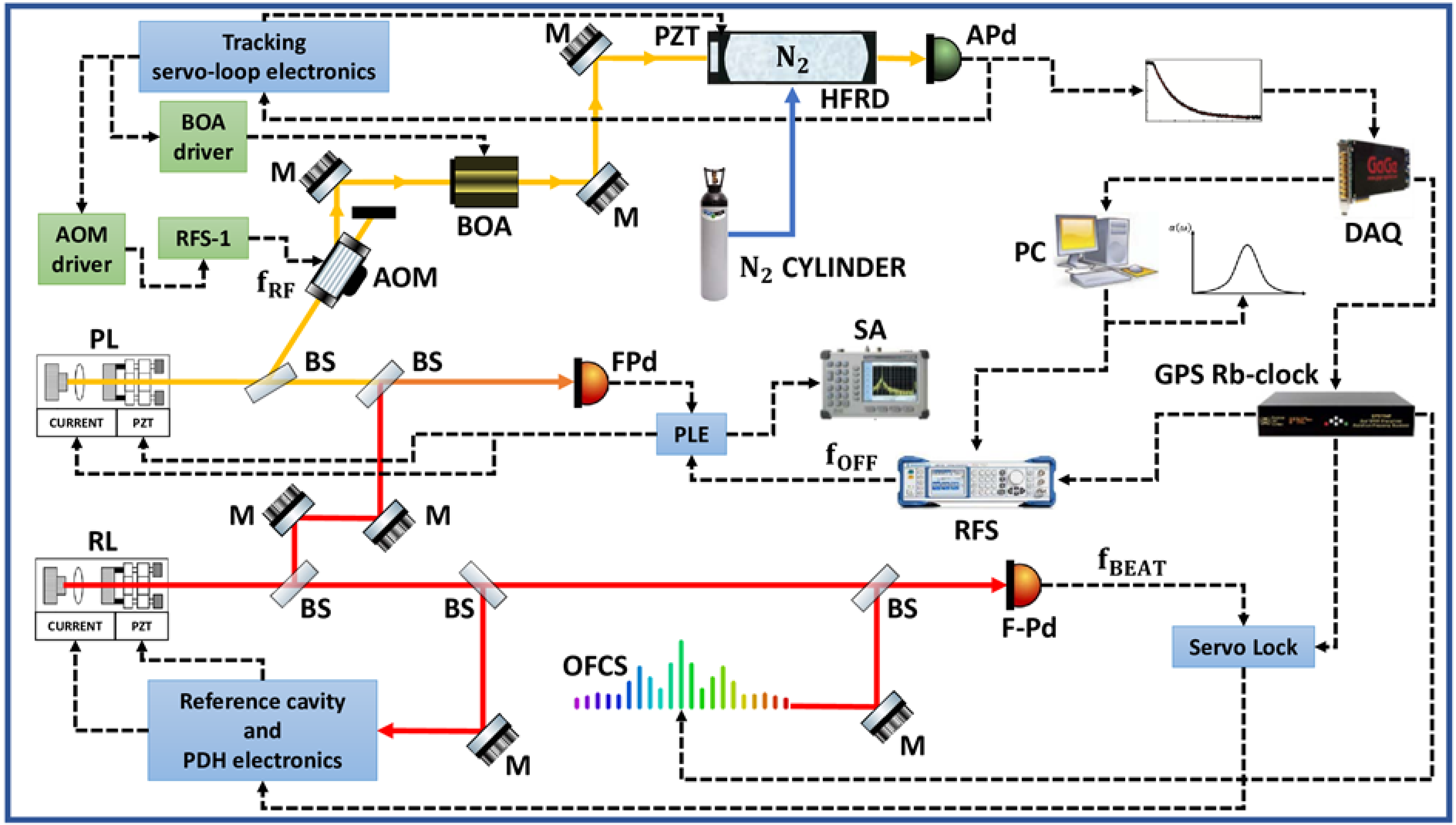

# A few pictures from the Lab

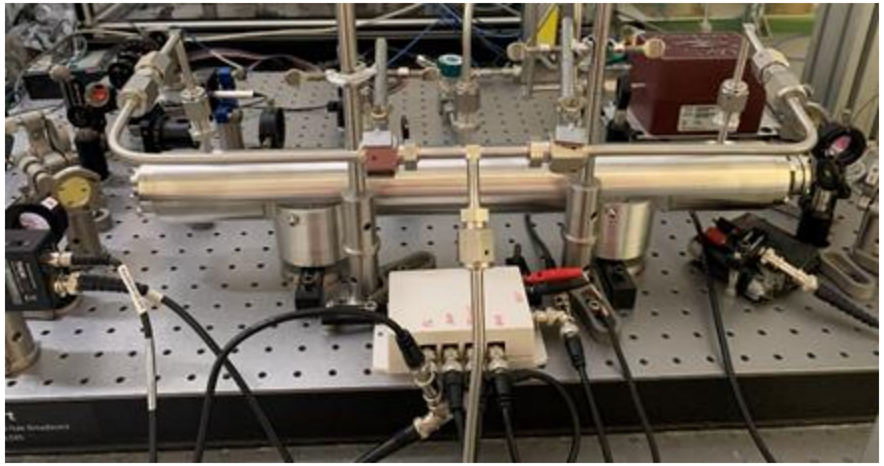

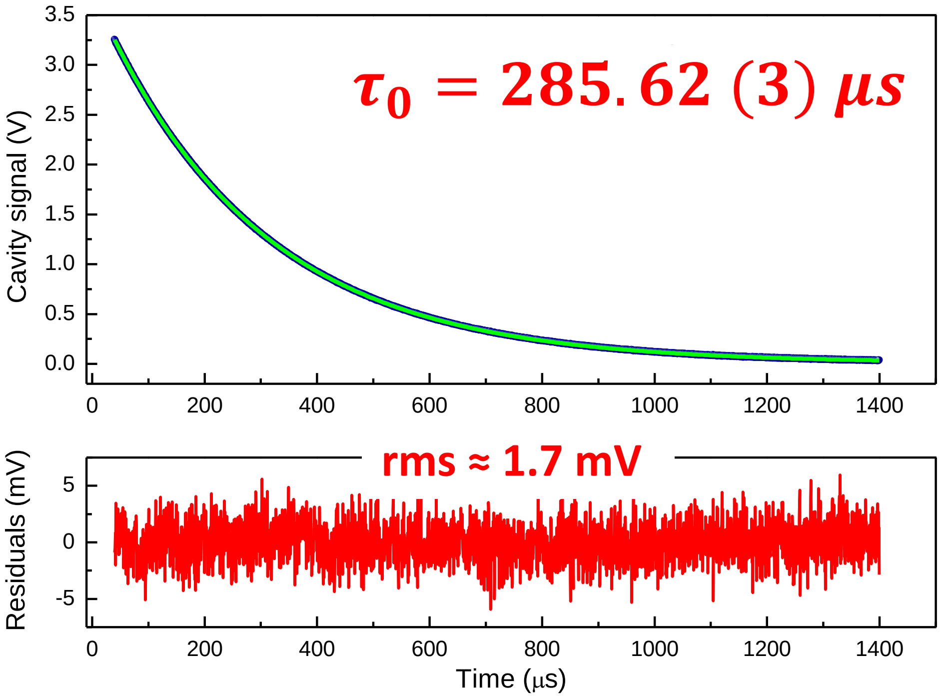


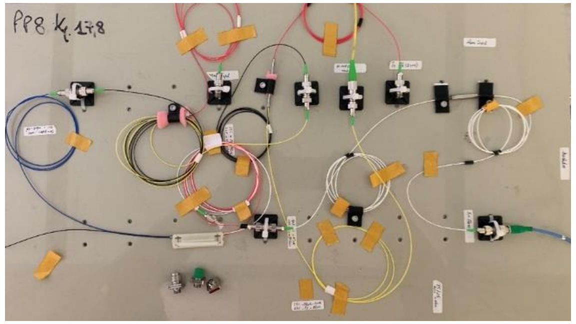

# The sensitivity of the CC-FS-CRDS spectrometer

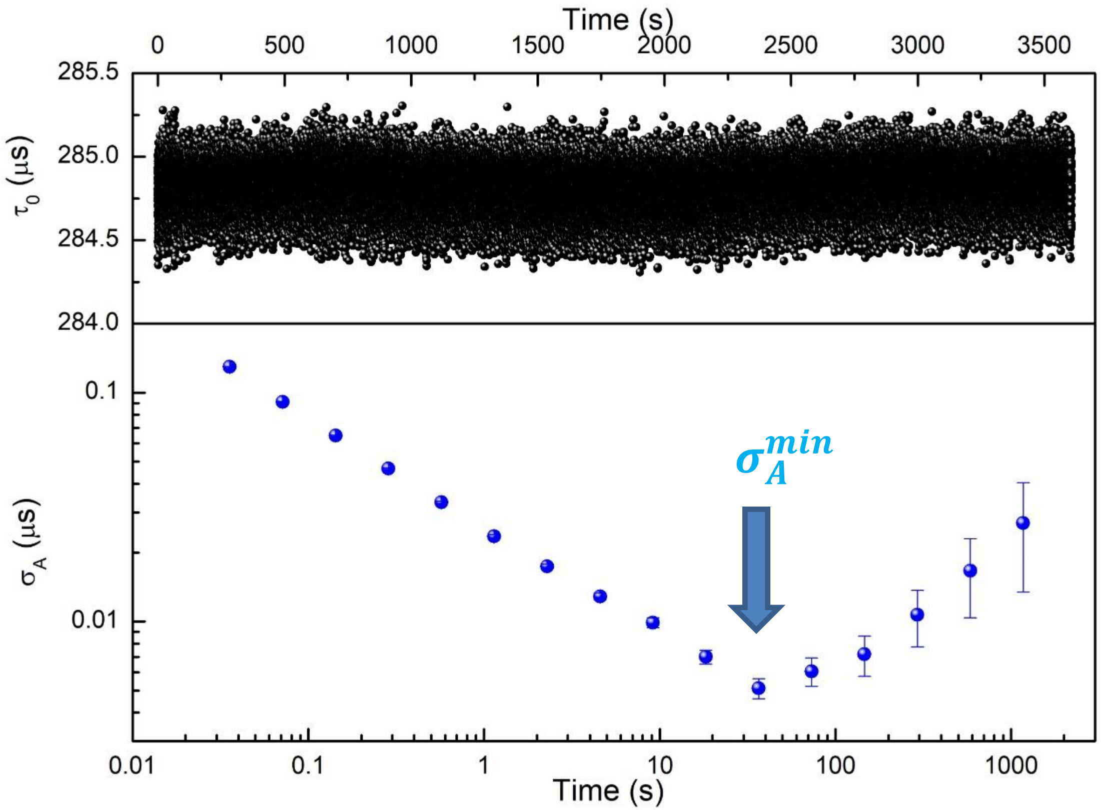


$$\alpha_{min} = \frac{\sigma_A^{min}}{c\tau_0^2} = 2.1 \times 10^{-12}\ cm^{-1}$$

$$NEA = \frac{\sigma_{\tau_0}}{c\tau_0^2}\sqrt{\frac{2}{f_{rate}}} = 1.4 \times 10^{-11}\ \frac{cm^{-1}}{\sqrt{Hz}}$$

Our sensitivity is a factor of 22 above the shot-noise limit!

Limiting factors: Mechanical, acoustic and thermal noises

Remedy: spectral averaging!!

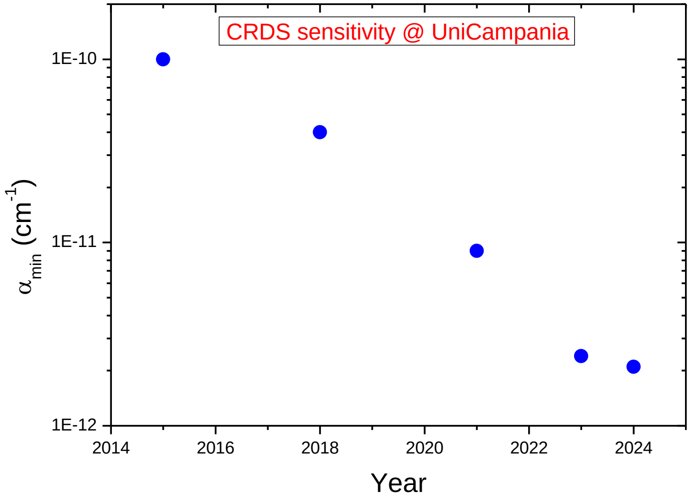

# Limit of detection

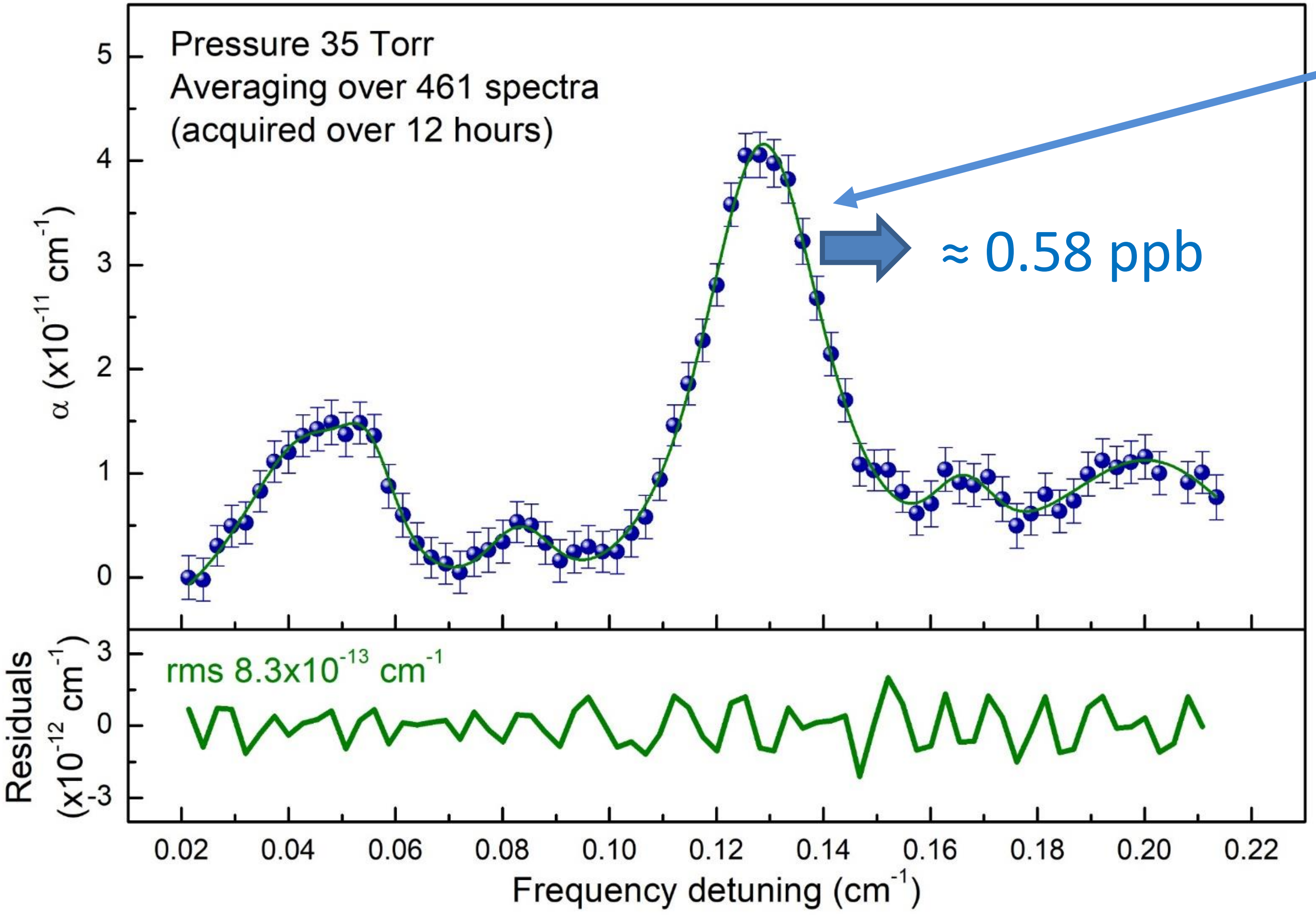


≈ 0.58 ppb

HDO transition
@ 7176.419270 cm$^{-1}$
S= 6.250x10$^{-25}$ cm/molecule

$$x_{W_{min}} = \frac{X_D \alpha_{rms} k_B T}{S g(0) p} \approx 12\ ppt$$

# Example of $H_2O$ mole fraction measurements

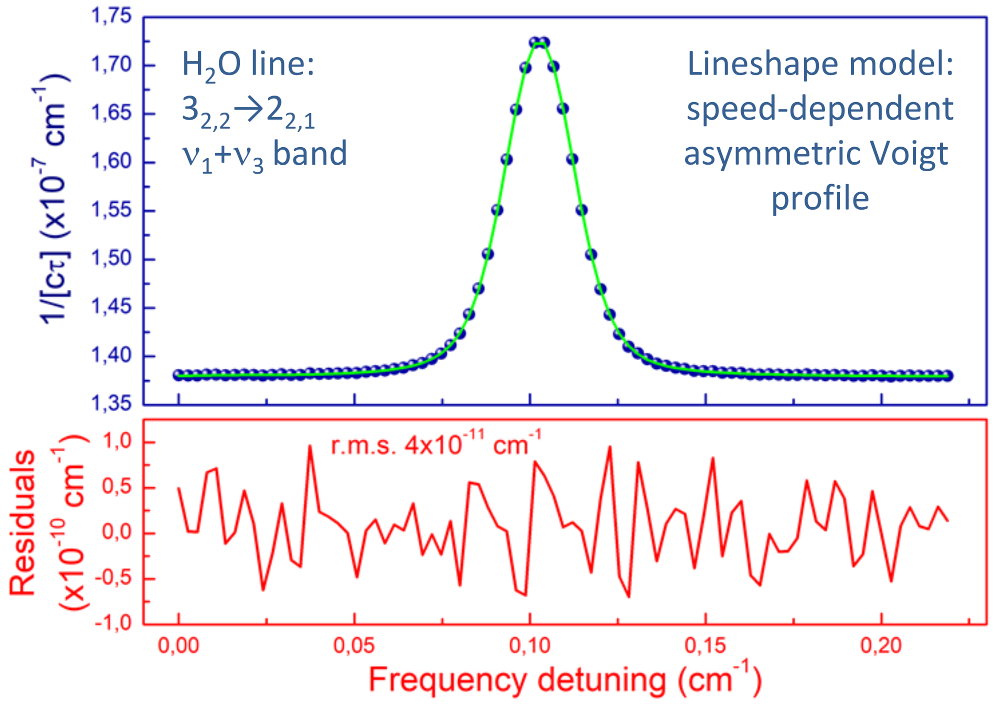


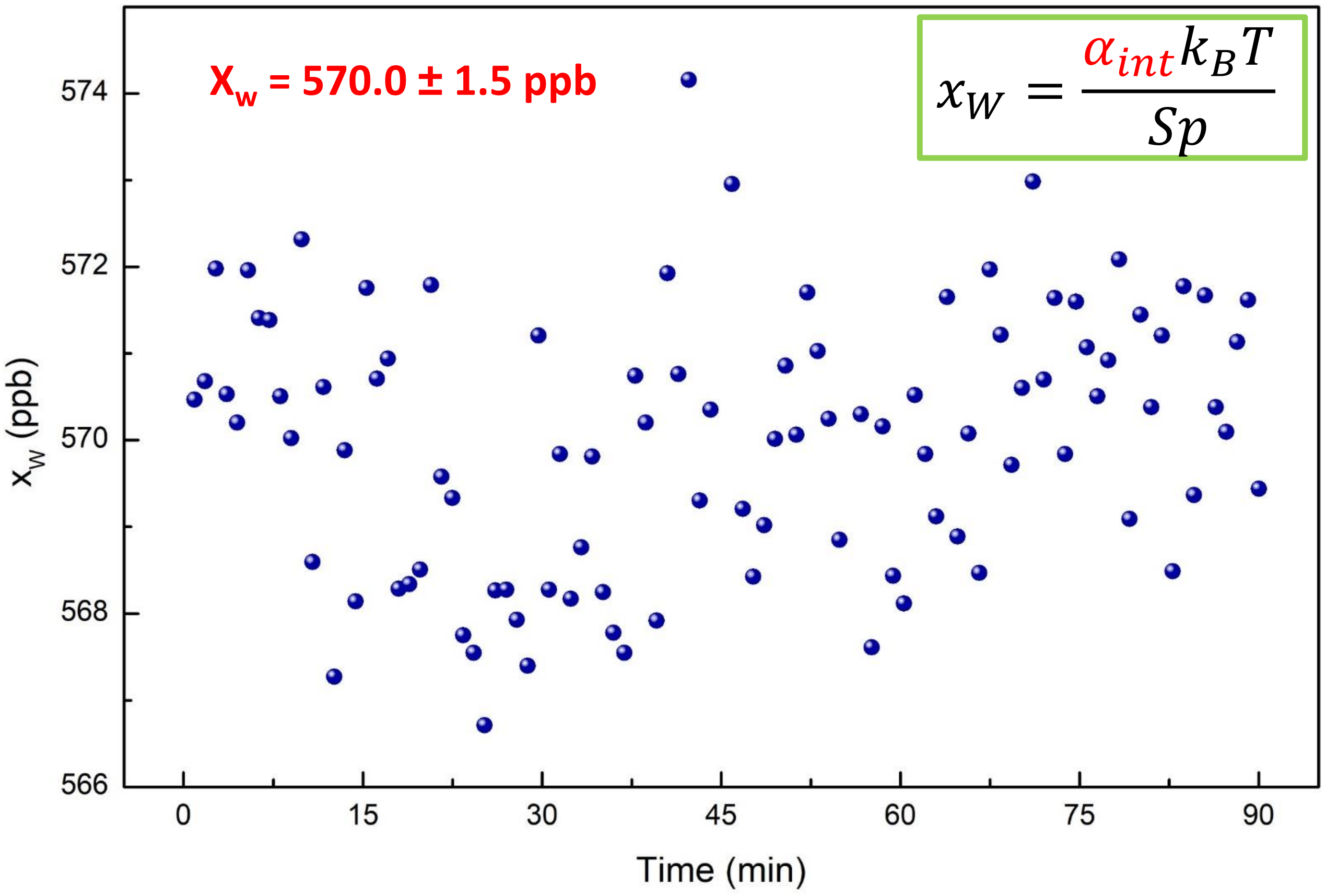


$$x_W = \frac{\alpha_{int} k_B T}{Sp}$$

Gas: 6.0 $N_2$ cylinder from Nippon Gases
Flux: 1100 sccm
Pressure (p): 32 Torr
Temperature (T): 296.6 K
Linestrength (S) value taken from: D. Lisak, D. K. Havey, and J. T. Hodges, Spectroscopic line parameters of water vapor for rotation-vibration transitions near 7180 $cm^{-1}$, Phys. Rev. A**79**, 052507 (2009)

# Selection of the lineshape model

Choice of the lineshape profile based upon:

- root mean square (rms) of the residuals;
- the **Akaike Information Criterion** ($q_{AIC}$);
- quality of fit parameter.

$$q_{AIC} = N_p\left[\ln \sigma_{fit}^2 + \ln 2\pi + 1\right] + +2\left(\boldsymbol{P_{fit}} + 1\right)$$

**Table 1**

$P_{fit}$, $q_{AIC}$, $QF$, and the rms values for the all the investigated line shape functions.

| $g(\nu - \nu_0)$ | rms (cm$^{-1}$) | $QF$ | $P_{fit}$ | $q_{AIC}$ |
|---|---|---|---|---|
| VP | $1.69 \times 10^{-9}$ | 141 | 5 | –2241.5 |
| MVP | $3.33 \times 10^{-10}$ | 715 | 6 | –2434.5 |
| SDVP | $2.84 \times 10^{-10}$ | 838 | 6 | –2453.6 |
| SDNGP | $2.80 \times 10^{-10}$ | 850 | 7 | –2453.3 |
| SDAVP | $2.75 \times 10^{-10}$ | 866 | 8 | –2453.4 |

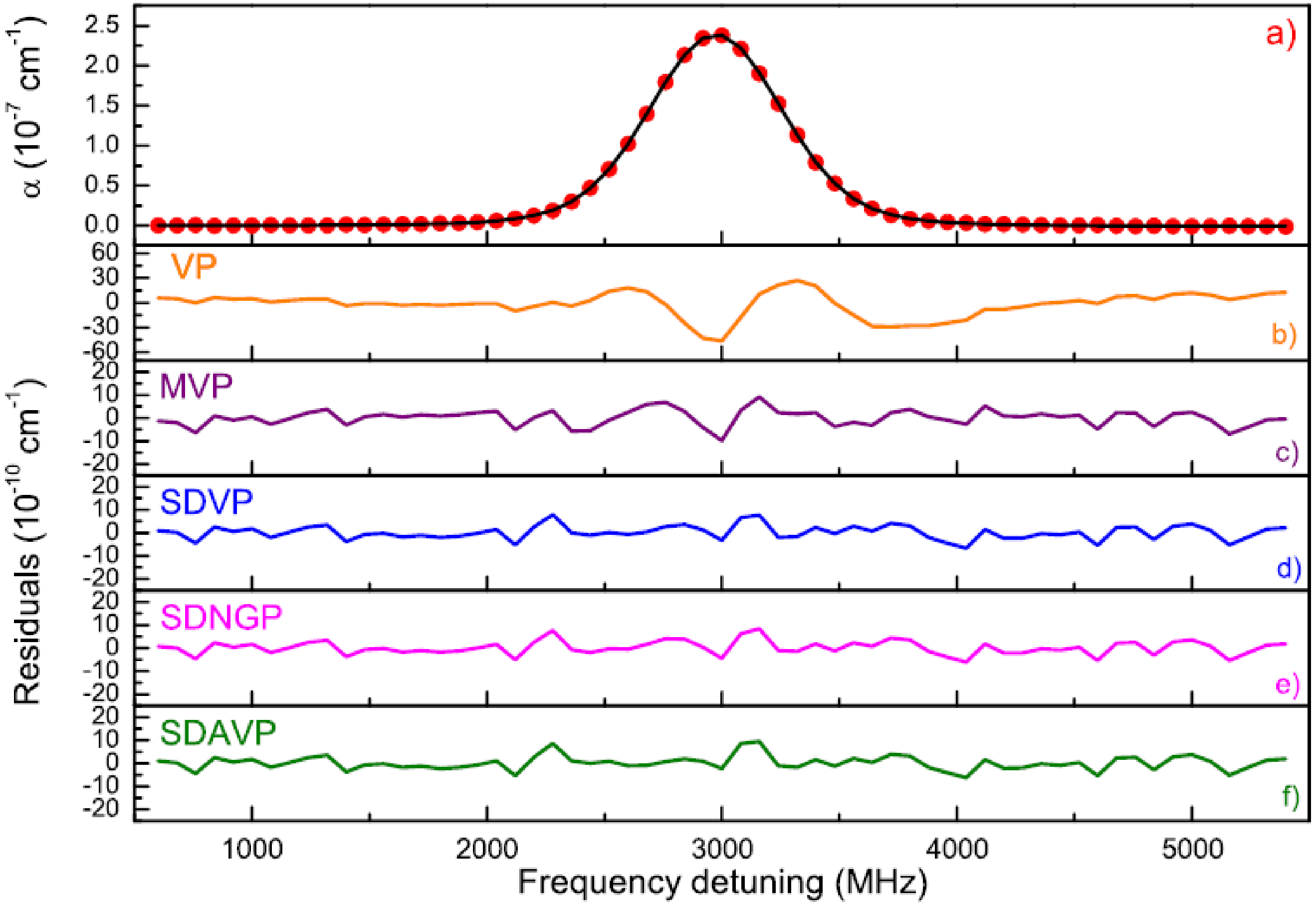


E. Fasci, M.A. Khan, V. D'Agostino, S. Gravina, V. Fernicola, L. Gianfrani, A. Castrillo: Water vapor concentration measurements in high purity gases by means of comb assisted cavity ring down spectroscopy. Sensors & Actuators A 362, 114632 (2023).

# Uncertainty budget

| Contribution (k=1) | Type A (%) | Type B (%) |
|---|---|---|
| Statistical | 0.3 | |
| Linestrength value | | 0.3 |
| Frequency axis | | Negligible |
| Laser scan width | | 0.1 |
| Spectral resolution (frequency step) | | 0.2 |
| Temperature | | 0.07 |
| Pressure | | 0.05 |
| Lineshape model | | 0.1 |
| Partition function | | 0.04 |
| Overall uncertainty | 0.5 % | |

# Comparison with a commercially-available CRDS instrument


HALO-RP Trace-Gas Moisture Analyzer

Main features:
LOD = 2 ppb
Accuracy = 4% of reading
Operating range = 0-10 ppm
Sample inlet pressure = 60 – 2000 Torr
Gas pressure in the RD-cell = 100 Torr
Empty-cavity $\tau \approx 110\ \mu s$

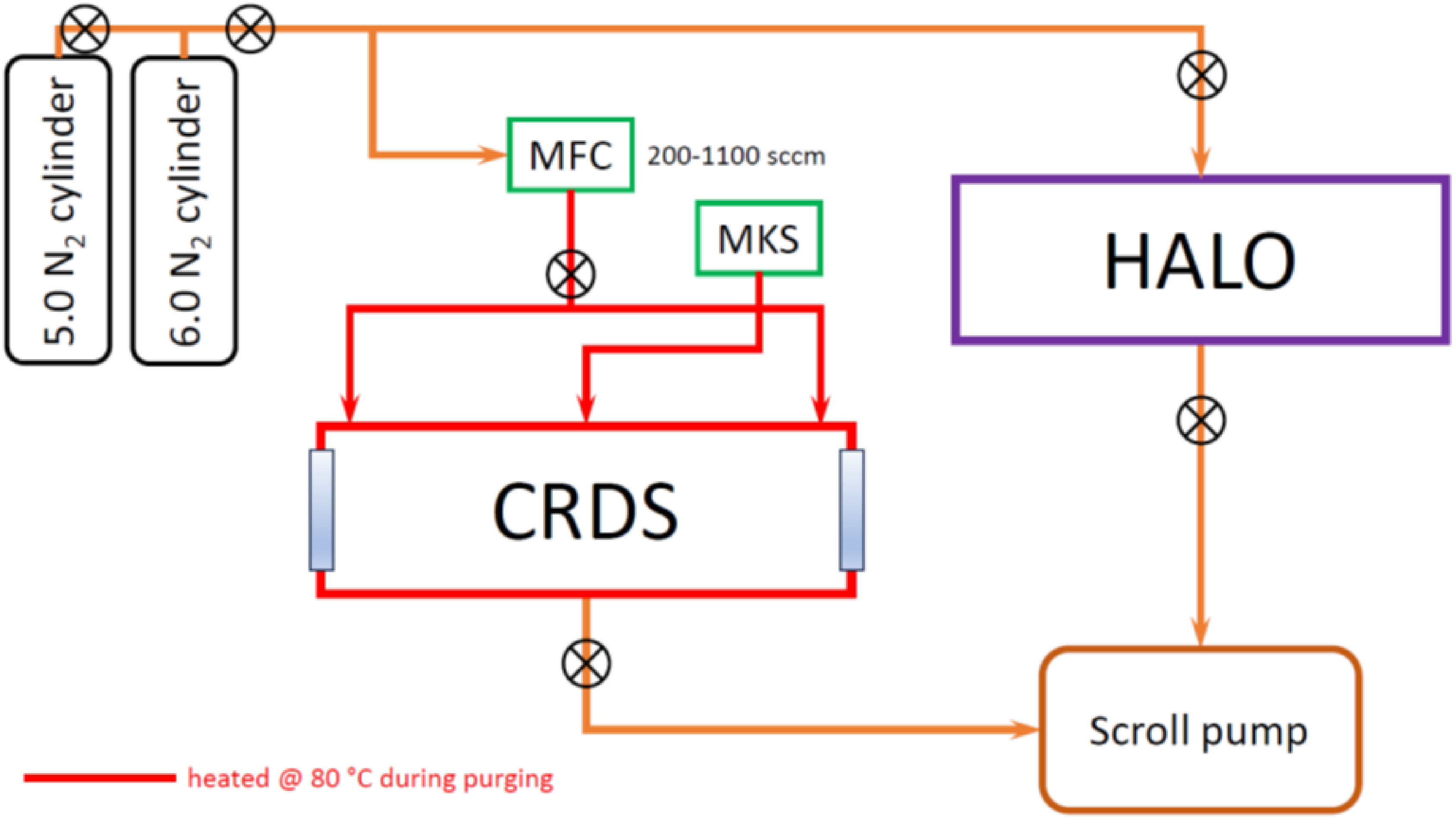

# Comparison with a commercially-available CRDS instrument

INRiM
ISTITUTO NAZIONALE
DI RICERCA METROLOGICA

Rugiada Cuccaro
& Vito Fernicola

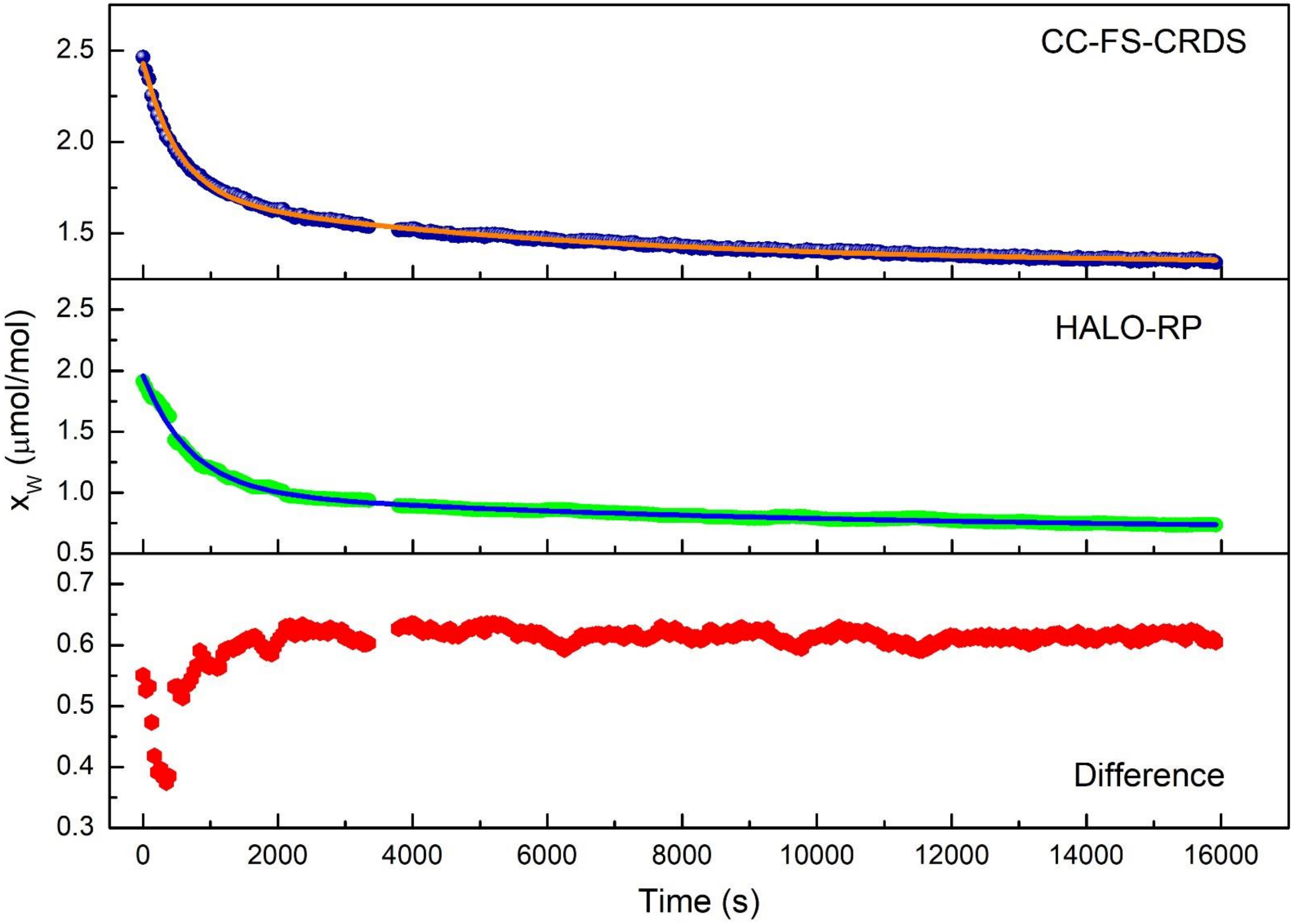

# Conclusions

- ✓ Continuous sub-ppm measurements of water mole fraction in ultra-high purity gases are possible with a relative uncertainty better than 1 %
- ✓ Spectroscopic measurements are characterized by an absolute, highly accurate and stable frequency axis
- ✓ The retrieval procedure is not sensitive to the gas mixture
- ✓ Our system acts as reference method to calibrate portable sensors and analyzers
- ✓ The system can be made much more compact and portable

# The AMP Group


Antonio Castrillo

Eugenio Fasci

# Thank you for your attention

EMPIR EURAMET
The EMPIR initiative is co-funded by the European Union's Horizon 2020 research and innovation programme and the EMPIR Participating States

# HALO-RP

| Performance | |
|---|---|
| Operating range | See table below |
| Detection limit (LDL, 3σ/24h) | See table below |
| Precision (1σ, greater of) | ± 1% or 1/3 of LDL |
| Accuracy (greater of) | ± 4% or LDL |
| Speed of response | < 3 minutes to 95% |
| Environmental conditions | 10°C to 40°C |
| | 30% to 80% RH (non-condensing) |
| Storage temperature | -10°C to 50°C |

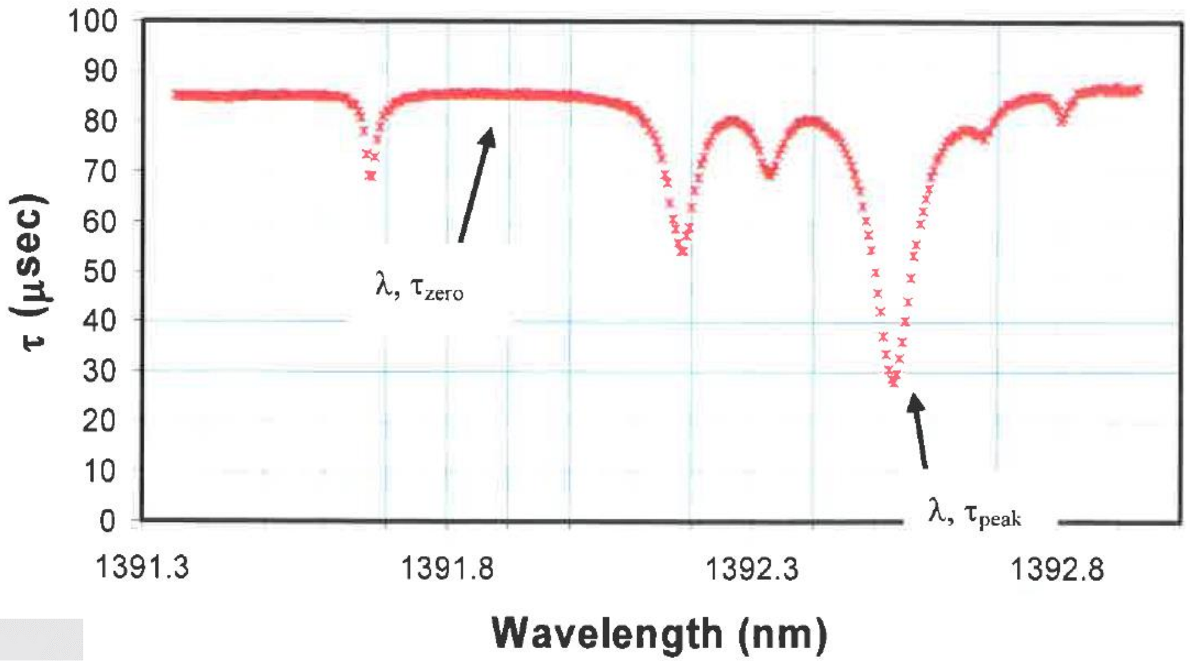


**HALO RP $H_2O$ — Trace Moisture Analyzer (Standard Model)**

| Performance, $H_2O$: | Range | LDL (3σ) | Precision (1σ) @ zero |
|---|---|---|---|
| In Nitrogen | 0 – 20 ppm | 1.5 ppb | 0.5 ppb |
| In Argon | 0 – 20 ppm | 1.5 ppb | 0.5 ppb |
| In Hydrogen‡ | 0 – 20 ppm | 1.5 ppb | 0.5 ppb |
| In Helium | 0 – 12 ppm | 1.0 ppb | 0.3 ppb |
| In Clean Dry Air (CDA) | 0 – 20 ppm | 1.5 ppb | 0.5 ppb |
| In HCl†,‡ | 0 – 25 ppm | 3 ppb | 1.0 ppb |
| in CO‡ | 0 – 20 ppm | 2 ppb | 0.7 ppb |
| In Phosphine‡ | 0 – 10 ppm | 9 ppb | 3 ppb |
| In Germane‡ | 0 – 18 ppm | 20 ppb | 7 ppb |

# Sources of type-B uncertainty